

# **Unique two-dimensional indium telluride templated by a rare wheel-shaped heterobimetallic Mn/In cluster**

Yao Fu,<sup>†,#</sup> Jian Zhou,<sup>\*,†,#</sup> Hua-Hong Zou,<sup>\*,†</sup> Filipe A. Almeida Paz,<sup>§</sup> Xing Liu,<sup>†</sup> and Lianshe

Fu<sup>§,§</sup>

<sup>†</sup>Chongqing Key Laboratory of Inorganic Functional Materials, College of Chemistry, Chongqing Normal University, Chongqing 401331, P. R. China

<sup>‡</sup>State Key Laboratory for Chemistry and Molecular Engineering of Medicinal Resources, School of Chemistry & Pharmacy of Guangxi Normal University, Guilin 541004, P. R. China

<sup>§</sup>Department of Chemistry, CICECO – Aveiro Institute of Materials, University of Aveiro, Campus Universitário de Santiago, 3810-193 Aveiro, Portugal.

<sup>·§</sup>Phantom-g, CICECO – Aveiro Institute of Materials, Department of Physics, University of Aveiro, 3810-193 Aveiro, Portugal

**General Remarks.** All analytical grade chemicals were obtained commercially and used without further purification. Elemental analyses (C, N and H) were performed using a PE2400 II elemental analyzer. IR spectra were obtained from a powdered sample pelletized with KBr on an ABB Bomen MB 102 series IR spectrophotometer in the range of 400–4000 $\text{cm}^{-1}$ . Energy-dispersive X-ray analysis (EDXA) was taken by using a JEOL JSM-6700F field-emission scanning electron microscope. Room-temperature optical diffuse reflectance spectra of the powdered samples were obtained with a Shimadzu UV-3150 spectrometer. The absorption ( $\alpha/S$ ) data were calculated from the reflectance using the Kubelka-Munk function,  $\alpha/S = (1 - R)^2/2R$ , where R is the reflection coefficient,  $\alpha$  is the absorption coefficient, and S is the scattering coefficient. PXRD patterns were obtained using a Bruker D8 Advance XRD diffractometer with Cu  $K\alpha$  radiation ( $\lambda = 1.54178 \text{ \AA}$ ). The magnetization of **1** was obtained with a Quantum Design MPMS-XL-5 magnetometer. PXRD patterns were obtained using a Bruker D8 Advance XRD diffractometer with Cu  $K\alpha$  radiation ( $\lambda = 1.54056 \text{ \AA}$ ). The working electrodes for photocurrent measurements were prepared by following processes. 8 mg of microcrystal sample was dispersed into a mixed solution of ethanol (200  $\mu\text{L}$ ) and Nafion (56  $\mu\text{L}$ ), followed by ultrasonic treatment for 0.5 h. Then, 210  $\mu\text{L}$  of the above slurry was coated onto the FTO glass (F-doped  $\text{SnO}_2$ ) with an effective area of 1  $\text{cm}^2$  and dried naturally at room temperature. The photocurrent experiment was performed on a CHI650E electrochemistry workstation in a three-electrode system, with the sample coated FTO glass as the working electrode, a Pt slice as the auxiliary electrode and a saturated calomel electrode (SCE) as the reference electrode. The supporting electrolyte solution was 0.1  $\text{mol}\cdot\text{L}^{-1}$   $\text{Na}_2\text{SO}_4$  aqueous solution (100 mL). A 450 W high pressure Xe lamp with 420 nm was used as the illumination source. The lamp was kept on continuously, and a manual shutter was used to block exposure of the sample to the light. The sample was typically irradiated at intervals of 100 s.

### *Crystal Structure Determination*

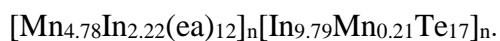
The intensity data of  $[\text{Mn}_{4.78}\text{In}_{2.22}(\text{ea})_{12}]_n[\text{In}_{9.79}\text{Mn}_{0.21}\text{Te}_{17}]_n$  were collected on a Bruker diffractometer-SMART-APEX II with graphite monochromated Mo  $K\alpha$  radiation ( $\lambda = 0.71073\text{\AA}$ ). Data reduction and absorption corrections were performed using the SAINT and SADABS software packages, respectively. The structure of  $[\text{Mn}_{4.78}\text{In}_{2.22}(\text{ea})_{12}]_n[\text{In}_{9.79}\text{Mn}_{0.21}\text{Te}_{17}]_n$  was solved by direct methods and refined by full-matrix least-squares methods on  $F^2$  using the SHELXL-2018 program package. The refinement with three octahedral metal sites occupied by three  $\text{Mn}^{2+}$  ions and one tetrahedral metal site occupied by one  $\text{In}^{3+}$  ion results in a molecular formula of  $[\text{Mn}_7(\text{ea})_{12}]_n[\text{In}_{10}\text{Te}_{17}]$ . The stoichiometry of  $[\text{Mn}_7(\text{ea})_{12}]_n[\text{In}_{10}\text{Te}_{17}]$  creates a charge of -2, which is not obviously rational. The U(iso) values of Mn2-4 are obviously smaller and the U(iso) value of In2 is obviously larger. When three octahedral metal sites are occupied by In6/Mn2, In7/Mn3 and In8/Mn4 atoms with occupation factors of 0.308/0.692, 0.334/0.666 and 0.469/0.531, respectively, and one tetrahedral metal site is occupied by In2/Mn5 atom with occupation factor of 0.893/0.107, the final  $R$  and  $wR$  factors ( $I > 2\sigma(I)$ ) are decreased from 0.0643/0.2225 to 0.0373/0.0973. So its formula was finally determined as  $[\text{Mn}_{4.78}\text{In}_{2.22}(\text{ea})_{12}]_n[\text{In}_{9.79}\text{Mn}_{0.21}\text{Te}_{17}]_n$ . The Te5, C6 and C8 atoms were disordered over site occupation factors of 0.89/0.11, 0.52/0.48 and 0.34/0.66, respectively. The non-hydrogen atoms were refined anisotropically. H atoms were placed in idealized locations and refined as riding. Technical details of data collections and refinement are summarized in Table S1.

Table S1 Crystallographic data for  $[\text{Mn}_{4.78}\text{In}_{2.22}(\text{ea})_{12}]_n[\text{In}_{9.79}\text{Mn}_{0.21}\text{Te}_{17}]_n$ .

formula	$\text{C}_{24}\text{H}_{72}\text{In}_{12}\text{Mn}_5\text{N}_{12}\text{O}_{12}\text{Te}_{17}$
$F_w$	4543.11
crystal system	Monoclinic
space group	$C2/c$
$a$ , $\text{\AA}$	25.7155(14)
$b$ , $\text{\AA}$	13.4091(7)

$c$ , Å	25.7626(15)
$\beta$ , deg	101.825(2)
$V$ , Å <sup>3</sup>	8695.0(8)
$Z$	4
$T$ , K	296(2)
Calcd density, Mg.m <sup>-3</sup>	3.470
abs coeff, mm <sup>-1</sup>	9.446
$F(000)$	7972
$2\theta(\text{max})$ , deg	55.76
Total reflns collected	31960
Unique reflns	10221
No. of param	399
$R1[I > 2\sigma(I)]$	0.0373
$wR2(\text{all data})$	0.0973
GOF on $F^2$	1.071

Table S2 The selected In-Te, In-O/N, Mn-Te and Mn-O/N bond lengths of



In-Te	2.6953(9)-2.9148(8)	In-O	2.07(3)-2.29(3)
In-N	2.26(3)-2.39(2)	Mn-O	2.09(3)-2.36(2)
Mn-N	2.14(3)-2.36(3)	Mn-Te	2.683(13)-2.855(11)

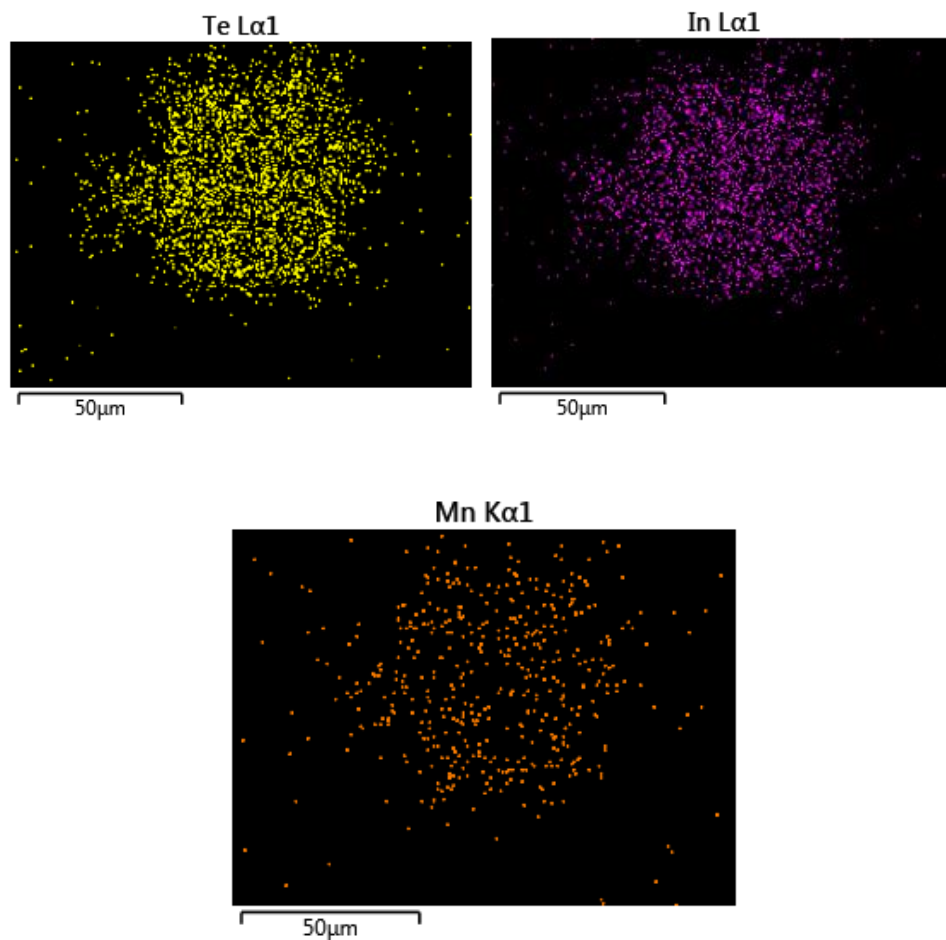


Figure S1 EDXA elemental mappings of Te, In and Mn in  $[\text{Mn}_{4.78}\text{In}_{2.22}(\text{ea})_{12}]_n[\text{In}_{9.79}\text{Mn}_{0.21}\text{Te}_{17}]_n$ .

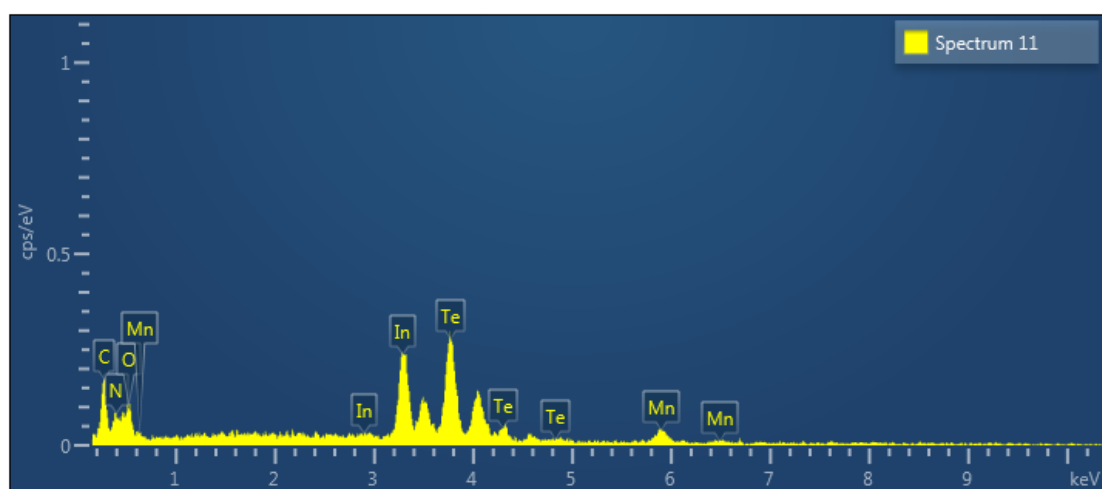


Figure S2 EDXA spectrum of  $[\text{Mn}_{4.78}\text{In}_{2.22}(\text{ea})_{12}]_n[\text{In}_{9.79}\text{Mn}_{0.21}\text{Te}_{17}]_n$ .

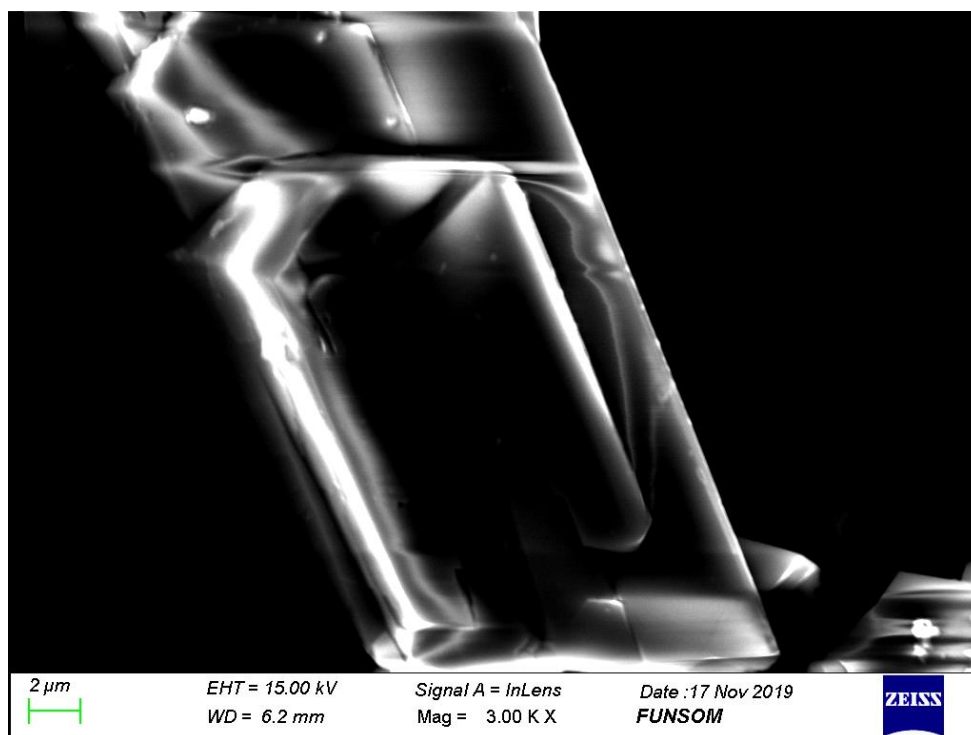


Figure S3 Scanning electron micrograph of  $[\text{Mn}_{4.78}\text{In}_{2.22}(\text{ea})_{12}]_n[\text{In}_{9.79}\text{Mn}_{0.21}\text{Te}_{17}]_n$ .

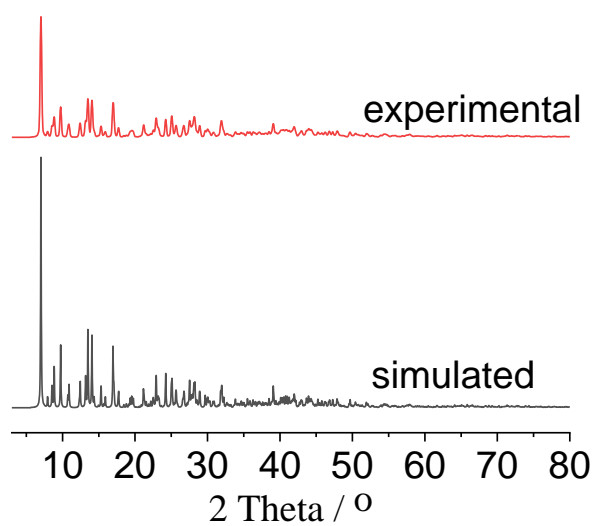


Figure S4 Simulated, and experimental powder XRD patterns of  $[\text{Mn}_{4.78}\text{In}_{2.22}(\text{ea})_{12}]_n[\text{In}_{9.79}\text{Mn}_{0.21}\text{Te}_{17}]_n$ .

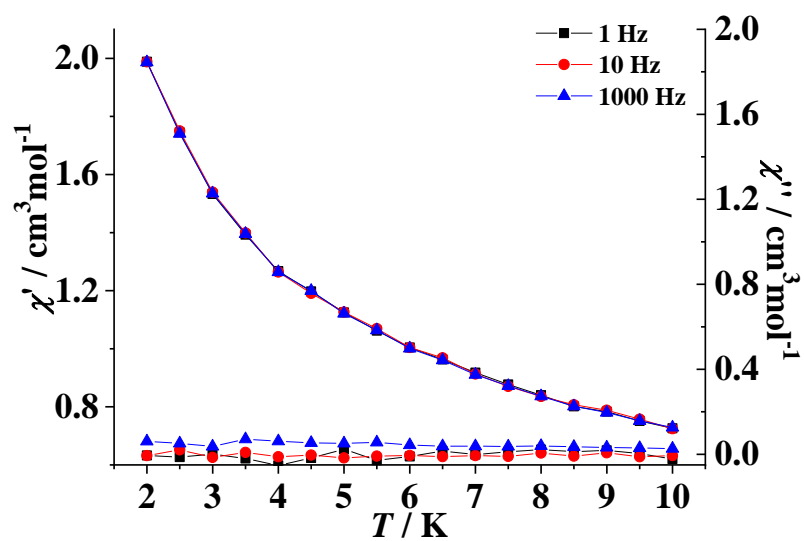


Figure S5 Temperature dependence of the in phase and out-of-phase signals of the ac susceptibility for  $[\text{Mn}_{4.78}\text{In}_{2.22}(\text{ea})_{12}]_n[\text{In}_{9.79}\text{Mn}_{0.21}\text{Te}_{17}]_n$  under a zero dc field ( $H_{ac} = 2.5$  Oe).

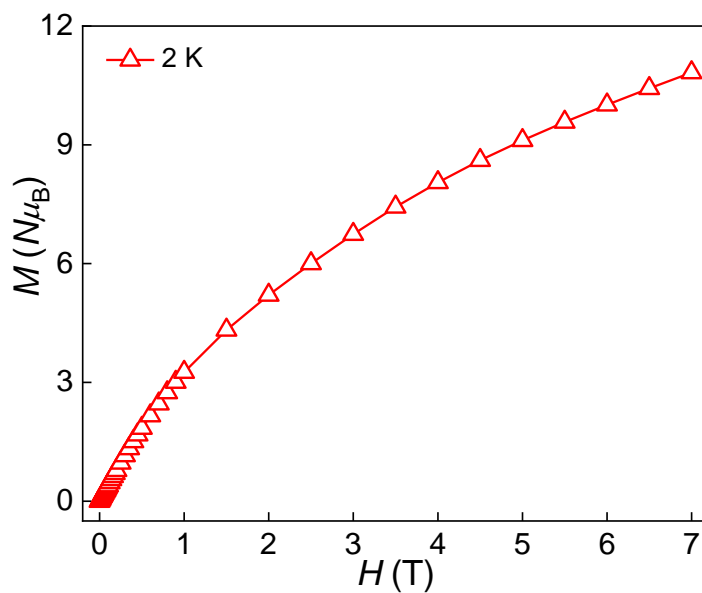


Figure S6 M versus H plot for  $[\text{Mn}_{4.78}\text{In}_{2.22}(\text{ea})_{12}]_n[\text{In}_{9.79}\text{Mn}_{0.21}\text{Te}_{17}]_n$ .